Journal of Physics G: Nuclear and Particle Physics

PAPER

Interaction of exotic states in a hadronic medium: the $Z_c(3900)$ case

To cite this article: L M Abreu *et al* 2024 *J. Phys. G: Nucl. Part. Phys.* **51** 095003

IOP Publishing Journal of Physics G: Nuclear and Particle Physics
J. Phys. G: Nucl. Part. Phys. **51** (2024) 095003 (19pp) https://doi.org/10.1088/1361-6471/ad66ec

Interaction of exotic states in a hadronic medium: the $Z_c(3900)$ case

L M Abreu[1,2,*], R O Magalhães[1], F S Navarra[3] and H P L Vieira[1]

[1] Instituto de Física, Universidade Federal da Bahia, Campus Universitário de Ondina, 40170-115, Bahia, Brazil
[2] Instituto de Física, Universidade de São Paulo, São Paulo, SP, Brazil
[3] Instituto de Física, Universidade de São Paulo, Rua do Matão 1371, 05508-090 Cidade Universitária, São Paulo, SP, Brazil

E-mail: luciano.abreu@ufba.br, rodrigomagalhaes@ufba.br, navarra@if.usp.br and hildeson.paulo@ufba.br

Received 10 April 2024, revised 26 June 2024
Accepted for publication 24 July 2024
Published 13 August 2024

Abstract

We investigate the interactions of the charged exotic state $Z_c(3900)$ in a hadronic medium composed of light mesons. We study processes such as $Z_c\pi \to D\bar{D}$, $Z_c\pi \to D^*\bar{D}^*$, $Z_c\pi \to D\bar{D}^*$ and the inverse ones. Using effective Lagrangians and form factors calculated with Quantum Chromodynamics (QCD) sum rules (treating the $Z_c(3900)$ as a tetraquark) we estimate the vacuum and thermally-averaged cross-sections of these reactions. We find that the $Z_c(3900)$ has relatively large interaction cross sections with the constituent particles of the hadronic medium. After that, we use the production and suppression cross sections in a rate equation to estimate the time evolution of the Z_c multiplicity. We include the Z_c decay and regeneration terms The coalescence model is employed to compute the initial Z_c multiplicity for the compact tetraquark configuration. Our results indicate that the combined effects of hadronic interactions, hydrodynamical expansion, decay and regeneration affect the final yield, which is bigger than the initial value. Besides, the dependence of the Z_c final yield with the centrality, center-of-mass energy and the charged hadron multiplicity measured at midrapidity $[\mathrm{d}N_{ch}/\mathrm{d}\eta(\eta<0.5)]$ is also investigated.

Keywords: exotic hadron states, heavy-ion collisions, hadron physics

* Author to whom any correspondence should be addressed.

1. Introduction

Hadron physics has definitively entered a new era since the early 2000s, with the discovery of new states that do not fit in the conventional definition of hadrons as $q\bar{q}$ mesons and qqq baryons. For a recent and comprehensive review we refer the reader to [1, 2]. Here we will focus on the $Z_c(3900)$ state. The charged components $Z_c(3900)^{\pm}$ were observed in 2013 by the BESIII collaboration as a peak in the invariant mass distribution of the system $\pi^{\pm}J/\psi$ in the $e^+e^- \to \pi^+\pi^+J/\psi$ reaction at the center-of mass energy of $\sqrt{s} = 4.16$ GeV [3]. The Belle collaboration has seen these states in e^+e^- collisions at $\sqrt{s}$ in the range 9.46–10.86 GeV [4]. Subsequent partial wave analysis has established their quantum numbers as $J^P = 1^+$ with statistical significance of more than 7.0σ [5]. In addition, the neutral component $Z_c(3900)^0$ was seen in the $\pi^0 J/\psi$ invariant mass of the $e^+e^- \to \pi^0\pi^0 J/\psi$ reaction at $\sqrt{s} = 4.23$, 4.26 and 4.36 GeV by BESIII [6] (see also [7, 8]); and at 4.17 GeV by using the CLEO-c detector [9]. According to the Review of Particle Physics (RPP) 2022 [10], the $Z_c(3900)$ averaged mass and width are respectively

$$M_{Z_c} = 3887.1 \pm 2.6 \ \text{MeV}, \ \Gamma_{Z_c} = 28.4 \pm 2.6 \ \text{MeV}. \tag{1}$$

These properties make the $Z_c(3900)$ incompatible with a mesonic structure and with the usual quark-model predictions, giving it the status of the first charged tetraquark state.

On the theoretical side there is a lively debate on the intrinsic nature of the $Z_c(3900)$, its production mechanisms and decay modes. Concerning its internal structure, several possibilities have been considered such as the hadronic molecule (see i.e. [11–26]); the compact tetraquark [27–32]; kinematical singularities such as threshold cusp effects [33, 34] or triangle singularities [35–37], and so on. In particular, in [25] the $Z_c(3900)$ was considered as a state belonging to the multiplet of S-wave hadronic molecules formed by a pair of ground state charmed and anticharmed mesons. Very recently, in [26] the $Z_c(3900)$ was treated as a $\pi J/\psi - D\bar{D}^*$ coupled-channel system in a covariant framework and the invariant masses extracted from the BESIII data and from lattice simulations were fitted. The probability of the $D\bar{D}^*$ component (calculated via compositeness condition) was found to be less than 0.5, suggesting that other hadronic components or compact quark state cores could be also important in the structure of the $Z_c(3900)$.

Clearly more contributions are welcome to shed light on the $Z_c(3900)$ properties and its internal structure. From the experimental side, heavy-ion collisions (HICs) appear as a promising environment. In these collisions, we expect to observe an enhancement in the multiplicity of exotic states, since a large number of heavy quarks are produced in the initial stages. After the collision and the formation of the quark–gluon plasma phase, the system expands and cools down, passing by a quark–hadron mixed phase and then reaching the hadronization point where a hot hadron gas is produced. During this transition the heavy quarks coalesce into bound states, mostly mesons and baryons, but also into multiquark states. Indeed, this expectation was recently confirmed by the observation of the most famous exotic state, the $X(3872)$, in Pb–Pb collisions at $\sqrt{s_{NN}} = 5.02$ TeV by the CMS Collaboration [38]. They found a prompt $X(3872)$ production rate which is about 10 times larger than that observed in p–p collisions. In addition, we should mention that the LHCb Collaboration reported the observation of $X(3872)$ in p-Pb collisions at $\sqrt{s} = 8.16$ TeV per nucleon [39]. On the theoretical side many studies appeared recently, such as those reported in [40–43]. This motivates us even more to continue to develop our program on exotics in HICs. Previously, the final yield of most of the conventional and some exotic hadrons in HICs has been estimated with the hadron statistical and coalescence models which do not include the interactions during the hadron gas phase [44]. However, our works have indicated that

hadronic interactions might strongly affect the final yield; see for example [45–56]. Any hadronic state can be suppressed due to its interaction with other hadrons of the medium, or be formed from the interaction of other particles. This issue becomes more crucial for the exotic states, because different structures (hadron molecule or compact tetraquark) have different spatial configurations, which lead to different interactions and cross sections.

In the present work we investigate the interactions of the $Z_c(3900)$ with the hadronic medium formed in HICs. In particular, we analyze the $Z_c(3900)$ suppression and production through processes such as $Z_c\pi \to D\bar{D}$, $Z_c\pi \to D^*\bar{D}^*$, $Z_c\pi \to D\bar{D}^*$, and the respective inverse reactions. Using effective Lagrangians, we estimate the vacuum and thermally-averaged cross-sections for these reactions, which are then employed in a kinetic equation in order to study the time evolution of the Z_c multiplicity. The small Z_c lifetime is also considered by including the Z_c decay and regeneration terms through an effective coupling, determined from the experimental data. The coalescence model is employed to compute the initial Z_c multiplicity. Besides, the dependence of the Z_c final yield on the centrality, center-of-mass energy and the charged hadron multiplicity measured at midrapidity $[\mathrm{d}N_{ch}/\mathrm{d}\eta(\eta < 0.5)]$ is also predicted.

Ideally, we would execute all the steps listed above for the $Z_c(3900)$ considered as meson molecule and also considered as a tetraquark. The cross sections and final yields would be different in each case and the latter would serve as a means to discriminate between the two configurations. After all this is one of the main questions in the field. However, at the moment we can not carry out the two independent calculations and compare the results because we do not know the coupling constants appearing in the interactions between meson molecules and light hadrons. Besides, very recent results indicate controversies in the context of meson-meson interaction approaches. One example is the discussion in [26], in which the compositeness coefficient of the $D\bar{D}^*$ component in the $Z_c(3900)$ state is less than 0.5, which suggests that other higher-mass hadronic components or compact quark state should be important in the intrinsic nature of the $Z_c(3900)$. Thus, we postpone the issue associated to the hadronic molecule interpretation to be addressed in the future.

For now, as it will be discussed, we only know these couplings for tetraquarks.

In the next section we will briefly describe the effective Lagrangian formalism and estimate the vacuum and thermally-averaged cross sections. In section 3 we present our approach for the evaluation of the Z_c multiplicity and discuss the results obtained. Finally, section 4 is devoted to the concluding remarks.

2. Interactions of $Z_c(3900)$ with pions

2.1. Effective Lagrangians and reactions

We are interested in the interactions of the $Z_c(3900)$ state (denoted as Z_c from now on) with a hadronic medium constituted of light hadrons. In principle we should include the interactions with all light mesons, such as π, K, η, ρ, ω, ...etc. However, from our previous experience with other multiquark states (such as the $\chi_{c1}(3872)$, $\chi_{c1}(4274)$, $Z_{cs}(3895)$, T_{cc}^{+}...) we learned that the pions are the most important particles and are enough for a first description of the hadronic gas. Therefore here we consider only the reactions involving the Z_c and pions. Specifically, for the case of Z_c suppression induced by a pion, we will look at the reactions $Z_c\pi \to D\bar{D}$, $Z_c\pi \to D^*\bar{D}^*$ and $Z_c\pi \to D\bar{D}^*$, taking into account the lowest-order Born contributions. In figure 1 the diagrams of these reactions are depicted. The corresponding transition amplitudes will be determined by means of the following effective Lagrangians [13, 19, 22, 52, 57–61]:

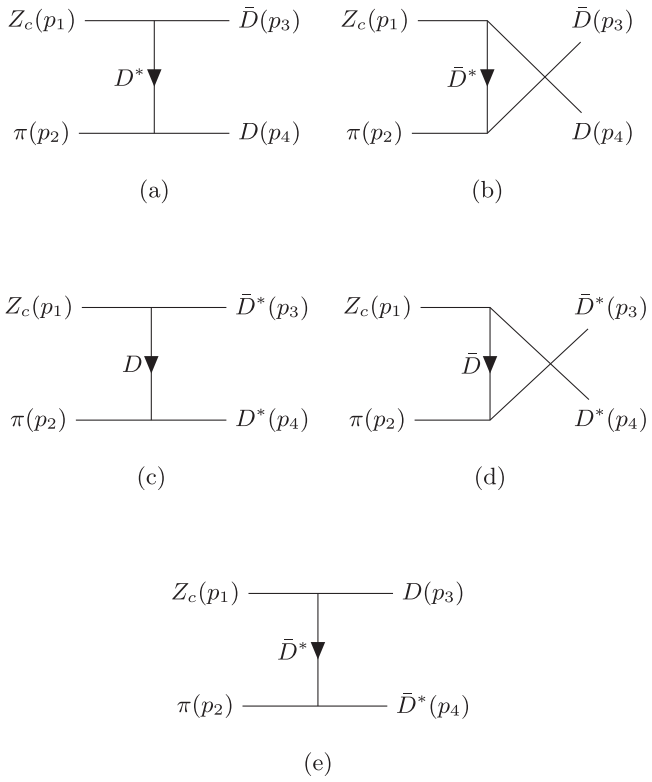

Figure 1. Diagrams contributing to the following processes: $Z_c\pi \to D\bar{D}$ (a) and (b), $Z_c\pi \to D^*\bar{D}^*$ (c) and (d), and $Z_c\pi \to D\bar{D}^*$ (e). The charges of the particles are not specified. The momenta of the particles in the initial (final) state are denoted as p_1 and p_2 (p_3 and p_4).

$$\begin{aligned}
\mathcal{L}_{Z_cDD^*} &= g_{Z_cDD^*} D^*_\mu \vec{Z}_c^{\,\mu} \cdot \vec{\tau} \bar{D} + H.c, \\
\mathcal{L}_{\pi DD^*} &= \mathrm{i} g_{\pi DD^*} D^*_\mu \vec{\tau} \cdot (\bar{D} \partial^\mu \vec{\pi} - \partial^\mu \bar{D} \vec{\pi}) + \mathrm{H.c.}, \\
\mathcal{L}_{\pi D^*D^*} &= -g_{\pi D^*D^*} \varepsilon^{\mu\nu\alpha\beta} \partial_\mu D^*_\nu \pi \partial_\alpha \bar{D}^*_\beta,
\end{aligned} \tag{2}$$

where g_{Z_cDD*}, $g_{\pi DD*}$ and $g_{\pi D*D*}$ are coupling constants; $\vec{\pi}$ and $\vec{Z}_c^{\,\mu}$ represent the pion and Z_c isospin triplets; $\vec{\tau}$ denote the Pauli matrices in the isospin space; $D(^*)$ and $\bar{D}(^*)$ are the isospin doublets for the pseudoscalar (vector) charmed mesons.

The Lagrangians are formally the same for tetraquarks and for meson molecules. However the coupling constants are different. In the case of tetraquarks they can be calculated with Quantum Chromodynamics (QCD) sum rules (QCDSR). QCDSR is a technique which makes use of a short distance expansion and hence it is appropriate to study systems of quarks which are typically less than 1 fm away from each other. Molecules, on the other hand, are systems which are typically larger than 1–2 fm and could be much larger. In the case of meson molecules the coupling constants can be calculated through the evaluation of triangular meson loops with effective theories as done, for example, in [62]. So in principle tetraquarks and molecules have the same Lagrangian but different coupling constants, which can be calculated. However, most of these calculations of couplings have not been done yet. The same considerations apply to the decay widths of tetraquarks and molecules. Fortunately, in the

case of the Z_c, we have all the ingredients for a tetraquark calculation. This is because the coupling constant appearing in the first line of equation (2) was calculated with QCD sum rules in [32] and the couplings appearing in the second and third lines of equation (2) were also calculated with QCDSR in [59]. Using these inputs and using the initial conditions given by the coalescence model for tetraquarks, we could obtain consistent results with all the inputs required for tetraquarks. Results for molecules could not be obtained and will be the subject of future work.

The transition amplitudes associated to the reactions shown in figure 1 can be determined from the effetive Lagrangians in equation (2) and are given by

$$\begin{aligned}\mathcal{M}(Z_c\pi \to D\bar{D}) &= \mathcal{M}^{(a)} + \mathcal{M}^{(b)},\\ \mathcal{M}(Z_c\pi \to D^*\bar{D}^*) &= \mathcal{M}^{(c)} + \mathcal{M}^{(d)},\\ \mathcal{M}(Z_c\pi \to D\bar{D}^*) &= \mathcal{M}^{(e)},\end{aligned} \tag{3}$$

where $M^{(i)}$ represents the amplitude coming from the specific process $(i) = (a),..., (e)$; these expressions are explicitly written as

$$\begin{aligned}\mathcal{M}^{(a)} &= g_{Z_cDD^*}g_{\pi DD^*}\epsilon_1^{\mu}(p_2 + p_4)^{\nu}\\ &\quad\times\left(g_{\mu\nu} - \frac{(p_1 - p_3)_{\mu}(p_1 - p_3)_{\nu}}{m_{D^*}^2}\right)\frac{1}{t - m_{D^*}^2},\\ \mathcal{M}^{(b)} &= -g_{Z_cDD^*}g_{\pi DD^*}\epsilon_1^{\mu}\times(p_2 + p_3)^{\nu}\\ &\quad\times\left(g_{\mu\nu} - \frac{(p_1 - p_4)_{\mu}(p_1 - p_4)_{\nu}}{m_{\bar{D}^*}^2}\right)\frac{1}{u - m_{\bar{D}^*}^2},\\ \mathcal{M}^{(c)} &= g_{Z_cDD^*}g_{\pi DD^*}\epsilon_1^{\mu}\epsilon_{3\mu}^{*}\epsilon_{4\nu}^{*}\left(\frac{1}{t - m_D^2}\right)(2p_2 - p_4)^{\nu},\\ \mathcal{M}^{(d)} &= -g_{Z_cDD^*}g_{\pi DD^*}\epsilon_1^{\mu}\epsilon_{4\mu}^{*}\epsilon_{3\nu}^{*}\left(\frac{1}{u - m_{\bar{D}}^2}\right)(2p_2 - p_3)^{\nu},\\ \mathcal{M}^{(e)} &= -g_{Z_cDD^*}g_{\pi D^*D^*}\varepsilon^{\mu\nu\alpha\beta}\epsilon_1^{\gamma}\epsilon_{4\nu}^{*}\\ &\quad\times\left(g_{\gamma\beta} - \frac{(p_1 - p_3)_{\gamma}(p_1 - p_3)_{\beta}}{m_{\bar{D}^*}^2}\right)\\ &\quad\times\frac{1}{t - m_{\bar{D}^*}^2}p_{4\mu}(p_4 - p_2)_{\alpha},\end{aligned} \tag{4}$$

where s, u and t are the Mandelstam variables, defined as $s = (p_1 + p_2)^2$, $t = (p_1 - p_3)^2$ and $u = (p_1 - p_4)^2$; and $\epsilon_i^{(*)} \equiv \epsilon^{(*)}(p_i)$ is the polarization vector associated to the corresponding vector meson.

Our model is indeed simple and certainly could be improved. However, we believe that it is already sufficient to set the scale of the relevant cross sections and to be used in the calculation of the Z_c multiplicity. The first simplifying assumption is to consider only the interaction between Z_c and pions, not including other mesons. This comes from our previous experience with several other exotic mesons interacting with a hadron gas. In all cases the pions give the most important contribution both for the cross section and, most importantly, for the thermal cross section, where the pion abundance in the gas is considered. The number of pions in the gas is by far much larger than the one of any other hadron species. The second

Table 1. Parameters of the form factors in the vertices with the mesons m_1, m_2 and m_3 [52, 59].

$m_1m_2m_3$	Form	A	B
$D\pi D^*$	I	126	11.9
$D^*\pi D^*$	II	4.8	6.8

simplifying assumption is to treat the interactions at tree level. Indeed these interactions can be treated much more rigorously using chiral perturbation theory, unitarization and two-body equations for the amplitudes. However, all this holds only for low energies, close to the thresholds. Here we are considering interaction energies determined by the temperature which is in the range 100–200 MeV. This is already too high to allow for the use of the more sophisticated approach mentioned above. On the other hand, the inclusion of form factors can cure some of the defficiencies of our effective theory, such as preventing the growth of the cross sections which would violate unitarity and also taking into account, to some extent, higher order corrections.

2.2. Form factors and coupling constants

In effective Lagrangian approaches we often use form factors to incorporate features associated to the finite size of the hadrons and also to prevent the artificial growth of the cross sections with the energy. A form factor can be obtained from the three-point function constructed with three meson currents. In QCD sum rules this three-point function is evaluated first writing the currents in terms of the quark fields, contracting them and performing an Operator Product Expansion of the resulting propagators. Then we evaluate the same three-point function using hadronic degrees of freedom. The sum rule is the equation obtained equating the two expressions of the same three-point function. In this equation the unknown is the form factor. More precisely, in a generic vertex of three mesons m_1, m_2 and m_3 the form factor is the function $g_{m_1\,m_2\,m_3}(p,\,p')$ (p and p' being the external 4-momenta) and it is evaluated in terms of the QCD parameters (quark masses and couplings) as well as of the meson masses and decay constants (see a detailed discussion in [52]). Here we benefit from previous works in which all the form factors required for the present calculation have been computed with QCDSR.

In the case of the vertices $D\pi D^*$ and $D^*\pi D^*$, the corresponding form factors have been calculated with QCDSR in [59]; they were parametrized as:

$$(I)\; g_{m_1m_2m_3}(Q^2) = \frac{A}{Q^2 + B} \tag{5}$$

and

$$(II)\; g_{m_1m_2m_3(Q^2)} = Ae^{-(Q^2/B)}, \tag{6}$$

where m_1 is the off-shell meson in the vertex and $Q^2 = -q^2$ its Euclidean four momentum; the parameters A and B are given in the table 1.

In [32] the $Z_c^+D^+\bar{D}^{*0}$ and $Z_c^+\bar{D}^0D^{*+}$ vertices were studied with QCDSR. The Z_c was treated as a genuine tetraquark $(\bar{c}\bar{q})(cq)$ with non-trivial color structure. The resulting form factor (valid for both vertices) was found to be

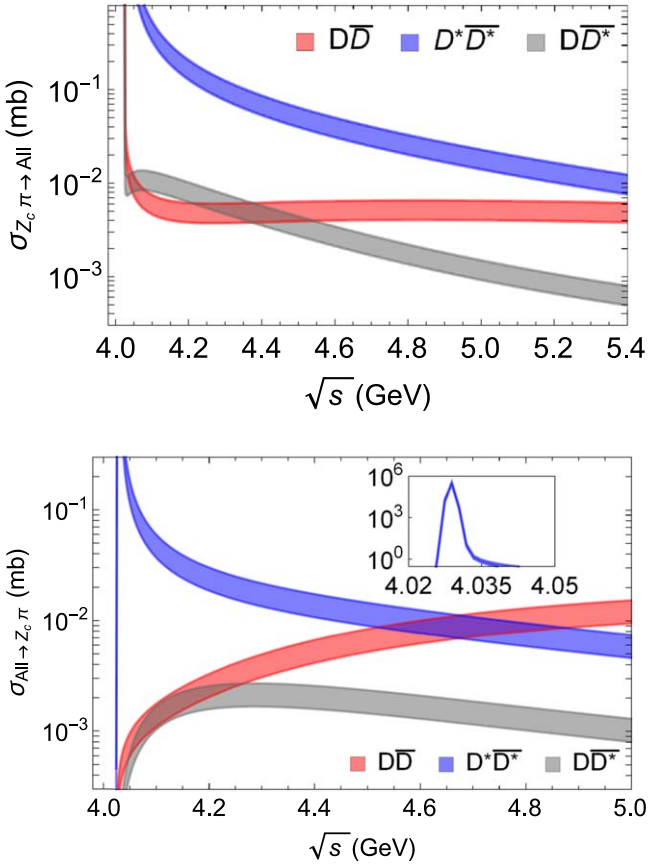

Figure 2. Top: cross sections for the suppression processes $Z_c\pi \to D^{(*)}\bar{D}^{(*)}$ as functions of $\sqrt{s}$. Bottom: cross sections for the corresponding inverse reactions. The inset figure shows the cross section for the $Z_c\pi \to D^*\bar{D}^*$ process in the energy region near 4.02 GeV. The bands represent the uncertainties coming from the largest and smallest values of the coupling constants in equation (8).

$$g_{Z_cDD^*}(Q^2) = \tilde{A}\ e^{-\tilde{B}\,Q^2} \tag{7}$$

with $\tilde{A} = 1.733$ GeV, $\tilde{B} = 0.076$ GeV^{-2}. Hence, from equations (5)–(7) the coupling constants can be fixed with $g_{m_1m_2m_3}(-m_1^2)$ and $g_{Z_cDD^*}(-m_D^2)$; they are:

$$\begin{aligned} g_{\pi DD^*} &= 14.0 \pm 1.5 \\ g_{\pi D^*D^*} &= (8.6 \pm 1.0)\ \text{GeV}^{-1}, \\ g_{Z_cDD^*} &= (2.5 \pm 0.3)\ \text{GeV}. \end{aligned} \tag{8}$$

The coupling $g_{Z_cDD^*}$ involving the neutral component Z_c^0 is not yet known. Notwithstanding, due to the proximity of the masses between the neutral and charged components of the Z_c, we will assume that the coupling $g_{Z_cDD^*}$ is also valid for the neutral component.

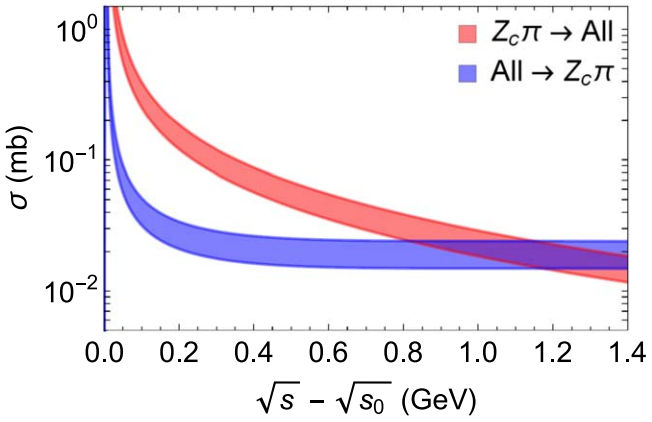

Figure 3. Sum of all cross-sections for the Z_c absorption and production processes as functions of $\sqrt{s} - \sqrt{s_0}$, where $\sqrt{s_0}$ is the corresponding threshold of each channel. All represents the sum $\sigma(Z_c\pi \to D\bar{D}) + \sigma(Z_c\pi \to D^*\bar{D}^*) + \sigma(Z_c\pi \to D\bar{D}^*)$ for the case of absorption processes and an equivalent expression for the inverse ones.

2.3. Cross sections

The isospin-spin-averaged cross section in the center of mass (CM) frame for a given reaction $ab \to cd$ in equation (3) is given by:

$$\sigma_{ab\to cd} = \frac{1}{64 g_a g_b \pi^2 s}\frac{|\vec{p}_{cd}|}{|\vec{p}_{ab}|}\int d\Omega \overline{\sum}|\mathcal{M}_{ab\to cd}|^2, \tag{9}$$

where $g_{a,b} = (2I_{a,b}+1)(2S_{a,b}+1)$ is the degeneracy factor of the particles in the initial state; s is the squared CM energy; $|\vec{p}_{ab}|$ and $|\vec{p}_{cd}|$ are the absolute values of the three-momenta in the CM frame of the initial and final particles; $\overline{\sum}$ denotes the summation over the spin and isospin of the initial and final states, which can be rewritten in the particle basis as

$$\sum_I |M_{ab\to cd}|^2 \to \sum_{Q_c,Q_d} |M^{(Q_c,Q_d)}_{ab\to cd}|^2. \tag{10}$$

with Q_c, Q_d being the explicit charges of the particles in the final state. For the inverse processes in which the $Z_c(3900)$ might be produced, i.e. $D\bar{D} \to Z_c\pi$, $D^*\bar{D}^* \to Z_c\pi$ and $D\bar{D}^* \to Z_c\pi$, the cross sections are calculated with the help of the detailed balance equation,

$$g_a g_b |\vec{p}_{ab}|^2 \sigma_{ab\to cd}(s) = g_c g_d |\vec{p}_{cd}|^2 \sigma_{cd\to ab}(s). \tag{11}$$

Now we can present and discuss the results. We remark that the estimates have been done with the isospin-averaged masses reported in [10]. Since the coupling constants are the same (see discussion in section 2.2), we assume that the charged $Z_c^{\pm}$ and neutral Z_c^0 components have identical contributions. So, the charges will not be explicit. Also, the results are presented in terms of bands associated to the smallest and largest possible values of the coupling constants.

In figure 2 we show the suppression processes $Z_c\pi \to D^{(*)}\bar{D}^{(*)}$ as functions of $\sqrt{s}$ and the corresponding inverse reactions. All the absorption processes are exothermic. The cross sections are very large close to the threshold and decrease with increasing energy $\sqrt{s}$. At moderate values of CM energy the reaction with final state $D^*\bar{D}^*$ yields the most relevant contribution, around one order of magnitude larger than the others. This might be partially

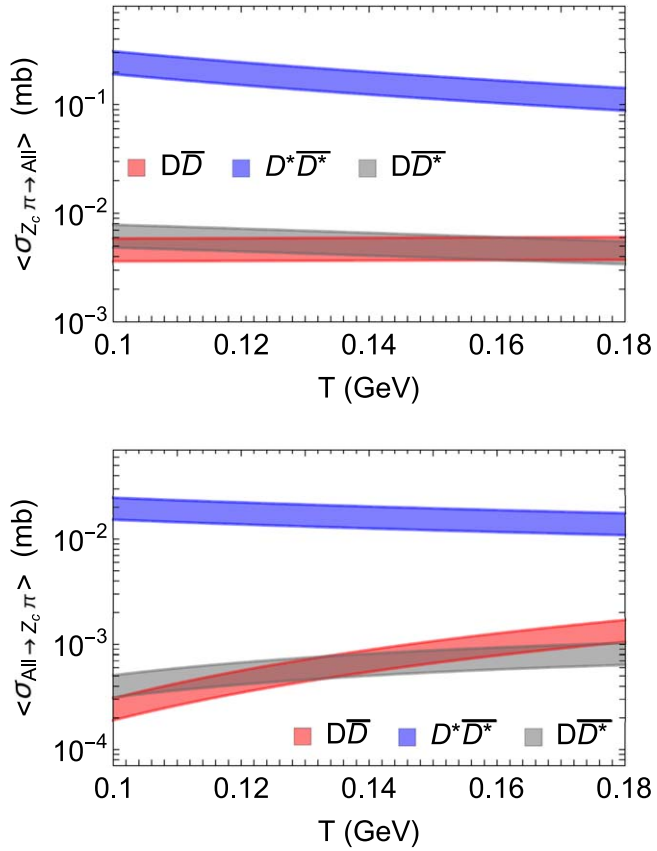

Figure 4. Top: thermally-averaged cross-sections of the processes $Z_c\pi \to D^{(*)}\bar{D}^{(*)}$ as functions of the temperature. Bottom: thermally-averaged cross-sections of the corresponding inverses reactions.

understood from the dynamics, as the exchanged charmed meson in this reaction is lighter than the one in other processes.

As we can see from figure 2, the Z_c production processes are endothermic and the cross sections tend to vanish near the threshold. Then they grow with $\sqrt{s}$ up to moderate energies. The channel with $D^*\bar{D}^*$ in the initial state presents a cusp close to the threshold, due to the small energy difference between the initial and final states. Comparing the Z_c absorption and production processes in the region of energies relevant for HICs ($\sqrt{s} - \sqrt{s_0} < 0.6$ GeV), the absorption cross sections are greater than the production ones. The difference comes from the phase space and the degeneracy factors encoded in equation (11). This feature becomes more evident in figure 3, where the sum of all cross-sections for the Z_c absorption and production processes are shown as a function of $\sqrt{s} - \sqrt{s_0}$ ($\sqrt{s_0}$ is the corresponding threshold of each channel).

2.4. Thermally-averaged cross sections

In view of our interest in a HIC environment, in which the medium effects become relevant and the Z_c may interact with light hadrons, it is necessary to evaluate the thermally-averaged cross sections, as the collision energy is related to the medium temperature. The cross-section

averaged over the thermal distributions of the particles participating in the reactions can be defined as the convolution of vacuum cross-sections and the momentum distributions. Strictly speaking, for a given reaction of the type $ab \to cd$, it is given by [44, 46, 51, 53, 57, 63]:

$$\begin{aligned}\langle \sigma_{ab\to cd} v_{ab}\rangle &= \frac{\int \mathrm{d}^3\mathbf{p}_a \mathrm{d}^3\mathbf{p}_b f_a(\mathbf{p}_a) f_b(\mathbf{p}_b)\sigma_{ab\to cd} v_{ab}}{\int \mathrm{d}^3\mathbf{p}_a \mathrm{d}^3\mathbf{p}_b f_a(\mathbf{p}_a) f_b(\mathbf{p}_b)} \\ &= \frac{1}{4\alpha_a^2 K_2(\alpha_a)\alpha_b^2 K_2(\alpha_b)} \int_{z_0}^{\infty} \mathrm{d}z K_1(z)\times \\ &\quad \times \sigma(s = z^2T^2)[z^2 - (\alpha_a + \alpha_b)^2] \\ &\quad \times [z^2 - (\alpha_a - \alpha_b)^2], \end{aligned} \tag{12}$$

where v_{ab} represents the initial relative velocity of the two interacting particles a and b; $f_i(_{pi})$ is the momentum distribution (here assumed to be the Bose–Einstein function); $\alpha_i = m_i/T$, where T is the temperature; $z_0 = \max(\alpha_a + \alpha_b, \alpha_c + \alpha_d)$; and K_1 and K_2 are the modified Bessel functions.

In figure 4 we plot the thermally-averaged cross-sections for the Z_c absorption and production processes as functions of the temperature. In the case of absorption, all the channels have a weak dependence with the temperature and the one with $D^*\bar{D}^*$ in the final state dominates. For the production processes, the temperature dependence is more prominent for the $D\bar{D}^*$ and $D\bar{D}$ channels, but the $D^*\bar{D}^*$ remains the most important contribution by at least one order of magnitude.

Here is one of the main conclusions of this study: as it happens to most of the other exotic states, the Z_c absorption processes are more important than the production reactions. This difference suggests that the hadronic medium may strongly affect the final number of produced Z_cs. In order to have a concrete prediction of this effect, the above cross sections will be used as input in the kinetic equation, whose solution yields the final Z_c multiplicity.

3. The $Z_c(3900)$ multiplicity

3.1. Time evolution

Now we move to the study of the time evolution of the Z_c multiplicity during the hadronic stage of heavy ion collisions. The formalism is the same used in our previous works, but for the sake of completeness we briefly describe it here. The thermally-averaged cross sections estimated in the previous section will be employed in the momentum-integrated evolution equation given by [45–48, 54]:

$$\begin{aligned}\frac{\mathrm{d}N_{Z_c}(\tau)}{\mathrm{d}\tau} &= \sum [\langle \sigma_{c\bar{c}\to Z_c\pi} v_{c\bar{c}}\rangle n_{\bar{c}}(\tau) N_c(\tau) - \langle \sigma_{Z_c\pi\to c\bar{c}} v_{Z_c\pi}\rangle n_\pi(\tau) N_{Z_c}(\tau)] \\ &\quad + \langle \sigma_{J/\psi\pi\to Z_c} v_{J/\psi\pi}\rangle n_\pi(\tau) N_{J/\psi}(\tau) - \langle \Gamma_{Z_c\to J/\psi\pi}\rangle N_{Z_c}(\tau), \end{aligned} \tag{13}$$

where $N_{Z_c}(\tau)$ denotes the multiplicity of Z_c at proper time τ; $n_c(\tau)$, $n_{\bar{c}}(\tau)$ and $n_\phi(\tau)$ are the number densities of charm and light mesons, respectively. The hadron gas is assumed to be in thermal equilibrium, and its constituents have their respective densities following the Boltzmann distribution

$$n_i(\tau) \approx \frac{1}{2\pi^2}\gamma_i g_i m_i^2 T(\tau) K_2\left(\frac{m_i}{T(\tau)}\right), \tag{14}$$

with γ_i, g_i, and m_i being the fugacity, degeneracy and mass of the particle i, respectively, and $T(\tau)$ the time-dependent temperature. The abundance $N_i(\tau)$ is obtained by multiplying $n_i(\tau)$ by the volume $V(\tau)$.

The last two lines of equation (13) describe the Z_c decay and its regeneration from the daughter particles. The Z_c has a large decay width and a lifetime shorter than that of the hadron gas phase ($\sim$10 fm/c). According to the RPP 2022 [10] the $Z_c \to D\bar{D}$ and $Z_c \to J/\psi\pi$ reactions have been seen. In [32] it was shown that the $Z_c \to J/\psi\pi$ is the most important decay channel. Thus we will include only this channel in our calculations. The other channel is also taken into account in the interactions of the Z_c with pions described in the previous section. Following the method summarized in [49, 64], we employ the effective Lagrangian

$$\mathcal{L}_{Z_c\psi\pi} = g_{Z_c\psi\pi}\partial_\mu\psi_\nu(\partial^\mu\pi Z_c^\nu - \partial^\nu\pi Z_c^\mu). \tag{15}$$

In this expression $g_{Z_c\psi\pi}$ is the coupling constant to be determined from the decay rate, written as

$$\Gamma_{Z_c\to J/\psi\pi}(\sqrt{s}) = \frac{1}{8\pi s}|p_{cm}(\sqrt{s})|\overline{\sum}|\mathcal{M}_\Gamma|^2, \tag{16}$$

where p_{cm} is the three-momentum in the center-of-mass frame, and $\mathcal{M}$ is the tree-level amplitude of the decay rate

$$\mathcal{M}_\Gamma = -g_{Z_c\psi\pi}p_{2\mu}\epsilon^*_{2\nu}[p_3^\mu\epsilon_1^\nu - p_3^\nu\varepsilon_1^\mu] \tag{17}$$

with the momenta of the states Z_c, J/ψ and π being given by p_1, p_2 and p_3, respectively. Using the experimental value of the Z_c decay width in the above formulas we determine the value of the coupling constant: $g_{Z_c\psi\pi} = (3.89 \pm 0.56)$ GeV. The Z_c decay width averaged over the thermal distribution is expressed by

$$\langle\Gamma_{Z_c\to J/\psi\pi}\rangle = \Gamma_{Z_c\to J/\psi\pi}(m_{Z_c})\frac{K_1(m_{Z_c}/T)}{K_2(m_{Z_c}/T)}. \tag{18}$$

In the case of regeneration process, the cross section is given by the spin-averaged relativistic Breit-Wigner approximation:

$$\sigma_{J/\psi\pi\to Z_c} = \frac{g_{Z_c}}{g_{J/\psi}g_\pi}\frac{4\pi}{p_{cm}^2}\frac{s\Gamma^2_{Z_c\to J/\psi\pi}}{(s - m^2_{Z_c})^2 + s\Gamma^2_{Z_c\to J/\psi\pi}}, \tag{19}$$

where g_{Z_c}, $g_{J/\psi}$ and g_π are the degeneracy factors of the Z_c, J/ψ and π respectively. This cross section is averaged over the thermal distribution in the same way as done in the previous section.

3.2. The expansion of the hadron gas

To describe the hadron gas evolution, in [65, 66] the authors proposed a model using the boost invariant Bjorken picture [67] with an accelerated transverse expansion. This model was further developed and applied in [47, 48, 54]. According to this picture the hadronic matter expands isentropically, with the proper-time dependence of the volume and temperature being parametrized as:

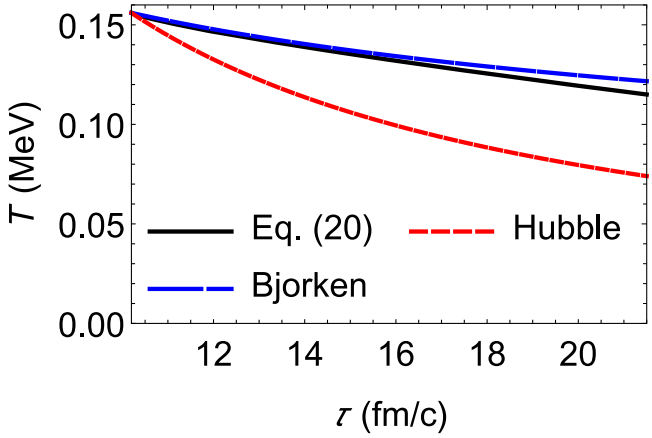

Figure 5. Time evolution of the temperature modelled as in equation (20), Hubble (equation (21)) and Bjorken (equation (22)) expansions.

Table 2. In the first three lines we list the parameters used in equation (20) for central Pb–Pb collisions at $\sqrt{s_{NN}} = 5.02$ TeV [44]. In the next two lines we list the multiplicities of the mesons and the quark masses used in the model. In the last line we show the frequency used in the coalescence model.

v_C(c)	a_C(c^2/fm)	R_C (fm)
0.5	0.09	11
τ_C (fm/c)	τ_H (fm/c)	τ_F (fm/c)
7.1	10.2	21.5
T_C (MeV)	T_H (MeV)	T_F (MeV)
156	156	115
$N_\pi(\tau_H)$	$N_D(\tau_H)$	$N_{D^*}(\tau_H)$
713	4.7	6.3
N_c	m_c [MeV]	m_q [MeV]
14	1500	350
ω_c [MeV]		
220		

$$V(\tau) = \pi\left[R_C + v_C(\tau - \tau_C) + \frac{a_C}{2}(\tau - \tau_C)^2\right]^2 \tau c,$$
$$T(\tau) = T_C - (T_H - T_F)\left(\frac{\tau - \tau_H}{\tau_F - \tau_H}\right)^{\frac{4}{5}}. \quad (20)$$

where R_C, v_C, a_C and T_C represent the transverse size, transverse velocity, transverse acceleration and temperature at the critical time τ_C, respectively; $T_H(T_F)$ is the temperature at the end of the mixed phase time $\tau_H(\tau_F)$. These parameters are fixed for a hadronic medium formed in central Pb–Pb collisions at $\sqrt{s_{NN}} = 5.02$ TeV according to [44], and are given in table 2.

To perform a comparison between distinct expansion models, we also consider that the hadron gas expands like a 3D Hubble expansion, which means that the temperature should be parametrized as [68, 69]

$$T_{Hu}(\tau) = T_H \frac{\tau_H}{\tau}. \tag{21}$$

The differences are seen in a more concrete way in figure 5, where we plot the time evolution of the temperature parametrized as in equations (20), (21) and also as in the original modelling of Bjorken expansion [67]

$$T_{Bj}(\tau) = T_H \left(\frac{\tau_H}{\tau}\right)^{1/3}. \tag{22}$$

We notice that the 3D Hubble expansion experiences a faster cooling than the other parametrizations, which present approximately the same behavior. In particular, while $T_{Hu}(\tau) \sim T_F$ at $\tau \sim 14\,\mathrm{fm/c}$, the Bjorken case gives $T_{Bj}(\tau) \sim T_F$ at $\tau \sim 21.5\,\mathrm{fm/c}$.

The multiplicities of the pions and charmed mesons are also shown in table 2, and are used to fit the fugacities in equation (14). In the case of charm quarks, since they are produced in the early stages of the collision, their total number (N_c) in charmed hadrons is assumed to be constant during the hadron gas phase, yielding a time-dependent charm-quark-fugacity factor $\gamma_c \equiv \gamma_c(\tau)$ in order to keep $N_c = n_c(\tau) \times V(\tau) = \text{const.}$

To determine the initial conditions for the rate equation (13) we employ the coalescence model. It has the relevant feature of carrying information concerning the intrinsic structure of the system (such as angular momentum and the type and number of constituent quarks), because the multiplicity of the hadronic state is computed from the convolution of the density matrix of its constituents and its Wigner Function. Accordingly, the yield of Z_c at τ_c can be written as [44]:

$$N_{Z_c}^{\mathrm{Coal}} \approx g_{Z_c} \prod_{j=1}^{n} \frac{N_j}{g_j} \prod_{i=1}^{n-1} \frac{(4\pi\sigma_i^2)^{\frac{3}{2}}}{V(1+2\mu_i T\sigma_i^2)} \times \left[\frac{4\mu_i T\sigma_i^2}{3(1+2\mu_i T\sigma_i^2)}\right]^{l_i}, \tag{23}$$

where g_j and N_j are the degeneracy and number of the jth constituent of the Z_c and $\sigma_i = (\mu_i\omega)^{-1/2}$. We assume that the hadron internal structure is represented by a harmonic oscillator, the parameter ω is the oscillator frequency and μ is the reduced mass. The angular momentum l_i is 0 for a S-wave. Here the Z_c is considered as a S-wave compact tetraquark, with the frequency, the quark numbers and masses summarized in table 2. Hence, putting all these parameters in equation (23), the initial Z_c multiplicity is

$$N_{Z_c}(\tau_H) = 2.1170 \times 10^{-4}. \tag{24}$$

3.3. Size of the system, CM energy and centrality

As discussed in [54], it is possible to relate the multiplicity to other relevant observables, such as the charged-particle pseudorapidity density at mid-rapidity, $[\mathrm{d}N_{ch}/\mathrm{d}\eta\ (|\eta| < 0.5)]$. Using the empirical formula [50]

$$T_F = T_{F0}\, e^{-b\mathcal{N}}, \tag{25}$$

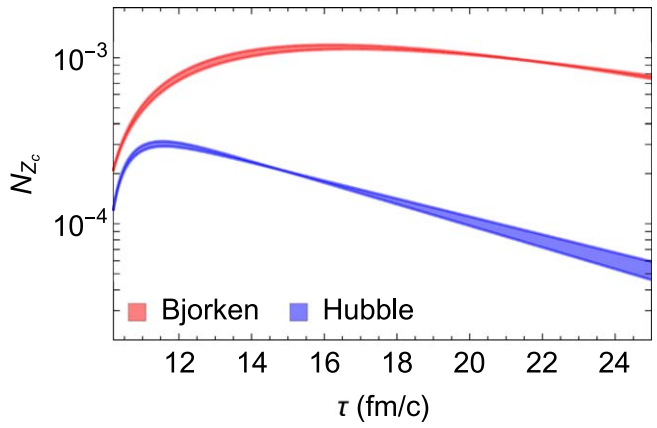

Figure 6. Abundance of $Z_c(3900)$ as a function of the proper time in central Pb–Pb collisions at $\sqrt{s_{NN}} = 5.02$ TeV, obtained with Bjorken and Hubble coolings.

where $T_{F0} = 132.5\,\text{MeV}$, $b = 0.02$ and $\mathcal{N} \equiv [\text{d}N_{ch}/\text{d}\eta(|\eta| < 0.5)]^{1/3}$. Assuming that the hadron gas undergoes a Bjorken-type cooling, then the freeze-out time τ_F and the freeze-out temperature can be related as follows [54]:

$$\tau_{F_{Bj}} = \tau_H \left(\frac{T_H}{T_{F0}}\right)^3 \text{e}^{3b\mathcal{N}}, \tag{26}$$

while in the case of a Hubble-type cooling it is given by

$$\tau_{Hu} = \tau_H \left(\frac{T_H}{T_{F0}}\right) \text{e}^{b\mathcal{N}}. \tag{27}$$

As we can see, $\mathcal{N}$ can be interpreted as an indirect measure of the duration of the hadronic phase, implying that a larger system (with a larger mass number A) will yield a larger charged-particle pseudorapidity density (bigger $\mathcal{N}$), generating a longer hadron phase (bigger τ_F). Hence, the use of equation (26) in (13) can be seen as an indirect estimate of the dependence of N_{Z_c} with the size of the system. Besides, $\mathcal{N}$ can also be related to the center-of-mass energy $\sqrt{s}$ and to the centrality of the collision. The empirical formulas relating $\mathcal{N}$ with $\sqrt{s}$ and the centrality are respectively given by (see a more detailed discussion about the obtention of these expressions in [54, 70]):

$$\left.\frac{\text{d}N_{ch}}{\text{d}\eta}\right|_{|\eta|<0.5} = -2332.12 + 491.69\log(220.06 + \sqrt{s}), \tag{28}$$

and

$$\begin{aligned}\left.\frac{\text{d}N_{ch}}{\text{d}\eta}\right|_{|\eta|<0.5} &= 2142.16 - 85.76x + 1.89x^2 - 0.03x^3 \\ &+ 3.67\times10^{-5}x^4 - 2.24\times10^{-6}x^5 \\ &+ 5.25\times10^{-9}x^6,\end{aligned} \tag{29}$$

where x represents %.

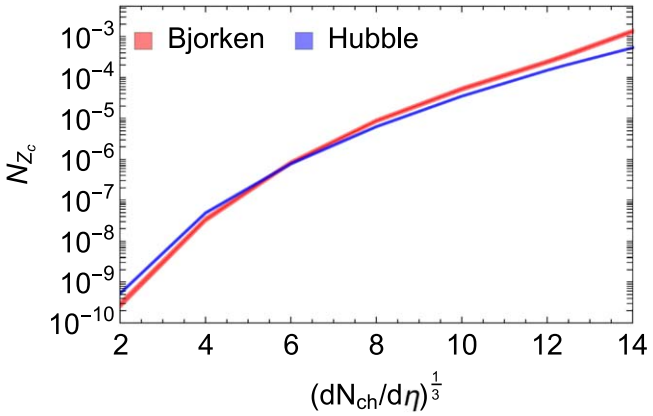

Figure 7. $Z_c(3900)$ multiplicity as a function of $\mathcal{N}$, obtained with Bjorken and Hubble coolings.

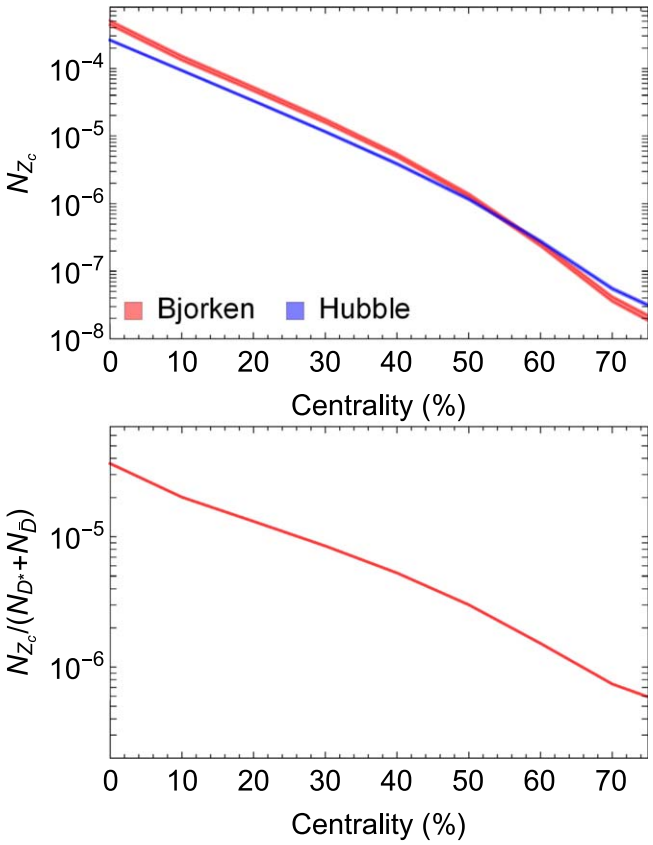

Figure 8. Top panel: $Z_c(3900)$ multiplicity as a function of the centrality, obtained with Bjorken and Hubble coolings. Bottom panel: ratio $N_{Z_c}/(N_{D^*} + N_{\bar{D}})$ as a function of the centrality, obtained with Bjorken cooling.

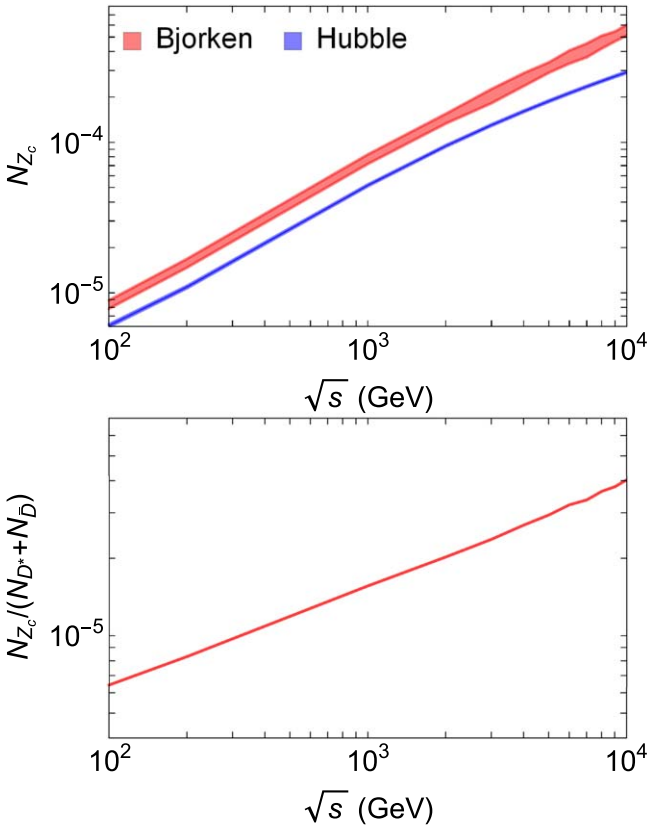

Figure 9. Top panel: $Z_c(3900)$ multiplicity as a function of the CM energy, obtained with Bjorken and Hubble coolings. Bottom panel: ratio $Z_c(3900)/(N_{D^*} + N_{\bar{D}})$ as a function of the CM energy, obtained with Bjorken cooling.

3.4. Results and discussion

The solution of equation (13) is presented in figure 6. As it can be seen, at the beginning of the hadron gas phase, the gain terms are dominant and generate an increase of the Z_c multiplicity. However, as the gas expands and cools down the Z_c production rate becomes smaller than the absorption rate, leading to a decrease of the abundance. Notwithstanding, at the freeze-out time the Z_c final yield is about four times larger than the initial value in the case of the Bjorken cooling. On the other hand, for the Hubble cooling the multiplicity decreases faster and its final value at the corresponding $\tau_F \sim 14\,\mathrm{fm/c}$ is larger by a factor of about 2.

In figure 7 we show the Z_c multiplicity as a function of $\mathcal{N}$. As expected, it grows with the size of the system, taking into account that that bigger systems like PbPb assume values of $\mathcal{N}$ of the order 10–12.5, where the Bjorken cooling gives larger N_{Z_c} and our approach is more reliable.

Finally, in the top panels of figures 8 and 9 we show the Z_c multiplicity as a function of the centrality and CM energy, obtained by using equations (26), (28) and (29) in (13). We notice that the Z_c final yield decreases from central to peripheral collisions and increases when the system reaches higher energies. To have a more complete description of the dependence of the Z_c yield with these observables, in the bottom panels of figures 8 and 9 we also plot the ratio $N_{Z_c}/(N_{D^*} + N_{\bar{D}})$ as a function of the centrality and CM energy. The results for the D^*

and $\bar{D}$ yields have been extracted from [71], which used the same collision conditions shown in table 2 within the Bjorken picture. Therefore, for coherence we present only the curves with the Z_c yield in the Bjorken cooling. Since the final yield $N_{D^*} + N_{\bar{D}}$ acquires a value of about 10 at $\sqrt{s_{NN}} \sim 5\,\text{TeV}$ in central collisions, then the ratio becomes approximately one order smaller than the magnitude of N_{Z_c} in this region.

4. Concluding remarks

Summarizing, the results discussed in the preceding sections suggest that the $Z_c(3900)$ state might suffer sizable interactions with the hadronic medium formed in HICs. First, we have studied the vacuum and thermally-averaged cross sections obtained for the Z_c absorption and production processes by comoving pions. They have been obtained from an effective Lagrangian formalism and form factors calculated with QCDSR considering the Z_c as a tetraquark state. We have found that the Z_c absorption processes are much more important than the production reactions. With the obtained cross sections we have studied the time evolution of the Z_c multiplicity, by using the production and suppression thermal cross sections in the rate equation. In this equation, the Z_c decay and regeneration terms were included. We have used the coalescence model to compute the initial Z_c multiplicity for the compact tetraquark configuration. Our results indicate that the combined effects of hadronic interactions, hydrodynamical expansion, decay and regeneration lead to an enhancement of the Z_c multiplicity at the end of the collision. As a final comment, it is also worth mentioning the findings reported in [37], where the triangle singularity interpretation of the Z_c was discussed in the context of HICs. The authors have argued that a HIC environment is the 'most universal eraser' of kinematic effects. The high temperatures affect the masses and widths of the particles participating in the process and if a triangle reaction is completed during the fireball lifetime, the triangle singularities will be washed out in the hot hadron gas phase. As a consequence, if the Z_c is generated by a $D_1 D^* D^*$ triangle loop, it will disappear at temperatures close to the deconfinement temperature. Hence, any future detection in HICs might be an indication that the Z_c is indeed a real hadron, while its absence points towards the singularity interpretation.

Acknowledgments

This work was partly supported by the Brazilian agencies CNPq/FAPERJ under the Project INCT-Física Nuclear e Aplicações (Contract No. 464898/2014-5); FAPESP; CNPq; and CAPES. The work of LMA is partly supported by the Brazilian agency CNPq under contracts 309950/2020-1, 400215/2022-5 and 200567/2022-5.

Data availability statement

All data that support the findings of this study are included within the article (and any supplementary files).

ORCID iDs

L M Abreu https://orcid.org/0000-0001-7408-1913

References

[1] Brambilla N, Eidelman S, Hanhart C, Nefediev A, Shen C-P, Thomas C E, Vairo A and Yuan C-Z 2020 *Phys. Rep.* **873** 1
[2] Wang X-Y, Li G, An C-S and Xie J-J 2022 *Phys. Rev.* D **106** 074026
[3] Ablikim M *et al* 2013 *Phys. Rev. Lett.* **110** 252001
[4] Liu Z *et al* 2013 *Phys. Rev. Lett.* **110** 252002
[5] Ablikim M *et al* 2017 *Phys. Rev. Lett.* **119** 072001
[6] Ablikim M *et al* 2015 *Phys. Rev. Lett.* **115** 112003
[7] Ablikim M *et al* 2015 *Phys. Rev. Lett.* **115** 222002
[8] Ablikim M *et al* 2014 *Phys. Rev. Lett.* **112** 022001
[9] Xiao T, Dobbs S, Tomaradze A and Seth K K 2013 *Phys. Lett.* B **727** 366
[10] Workman R L *et al* 2022 *Prog. Theor. Exp. Phys.* **2022** 083C01
[11] Guo F-K, Hidalgo-Duque C, Nieves J and Pavón Valderrama M 2013 *Phys. Rev.* D **88** 054007
[12] Chen H-X, Chen W, Liu X and Zhu S-L 2016 *Phys. Rep.* **639** 1
[13] Chen D-Y and Dong Y-B 2016 *Phys. Rev.* D **93** 014003
[14] Sun Z-F, He J, Liu X, Luo Z-G and Zhu S-L 2011 *Phys. Rev.* D **84** 054002
[15] Sun Z-F, Luo Z-G, He J, Liu X and Zhu S-L 2012 *Chin. Phys.* C **36** 194
[16] Wang Z-G and Huang T 2014 *Eur. Phys. J.* C **74** 2891
[17] Chen W, Steele T, Chen H-X and Zhu S-L 2015 *Phys. Rev.* D **92** 054002
[18] Wilbring E, Hammer H-W and Meißner U-G 2013 *Phys. Lett.* B **726** 326
[19] Dong Y, Faessler A, Gutsche T and Lyubovitskij V E 2013 *Phys. Rev.* D **88** 014030
[20] Dong Y, Faessler A, Gutsche T and Lyubovitskij V E 2014 *Phys. Rev.* D **89** 034018
[21] Li G, Liu X H and Zhou Z 2014 *Phys. Rev.* D **90** 054006
[22] Gutsche T, Kesenheimer M and Lyubovitskij V E 2013 *Phys. Rev.* D **90** 094013
[23] Guerrieri A and Pilloni A 2015 *Phys. Lett.* B **746** 194
[24] Ke H-W, Wei Z-T and Li X-Q 2013 *Eur. Phys. J.* C **73** 2561
[25] Ji T, Dong X-K, Albaladejo M, Du M-L, Guo F-K and Nieves J 2022 *Phys. Rev.* D **106** 094002
[26] Yan L-W, Guo Z-H, Guo F-K, Yao D-L and Zhou Z-Y 2024 *Phys. Rev.* D **109** 014026
[27] Maiani L, Piccinini F, Polosa A and Riquer V 2005 *Phys. Rev.* D **71** 014028
[28] Maiani L, Riquer V, Faccini R, Piccinini F, Pilloni A and Polosa A 2013 *Phys. Rev.* D **87** 111102
[29] Ali A, Hambrock C and Wang W 2012 *Phys. Rev.* D **85** 054011
[30] Deng C, Ping J, Huang H and Wang F 2014 *Phys. Rev.* D **90** 054009
[31] Wang Z-G and Zhang J-X 2018 *Eur. Phys. J.* C **78** 14
[32] Dias J M, Navarra F, Nielsen M and Zanetti C 2013 *Phys. Rev.* D **88** 016004
[33] Chen D-Y, Liu X and Matsuki T 2013 *Phys. Rev.* D **88** 036008
[34] Swanson E S 2015 *Phys. Rev.* D **91** 034009
[35] Liu X-H, Oka M and Zhao Q 2016 *Phys. Lett.* B **753** 297
[36] Szczepaniak A P 2015 *Phys. Lett.* B **747** 410
[37] Llanes-Estrada F J and Abreu L M 2022 *PoS PANIC2021* **380** 181
[38] Sirunyan A M *et al* (CMS) 2022 *Phys. Rev. Lett.* **128** 032001
[39] Aaij R *et al* (LHCb) 2024 *Phys. Rev. Lett.* **132** 242301 arXiv:2402.14975
[40] Esposito A, Ferreiro E G, Pilloni A, Polosa A D and Salgado C A 2021 *Eur. Phys. J.* C **81** 669
[41] Wu B, Du X, Sibila M and Rapp R 2021 *Eur. Phys. J.* A **57** 122
Wu B, Du X, Sibila M and Rapp R 2021 *Eur. Phys. J.* A **57** 314
[42] Zhang H, Liao J, Wang E, Wang Q and Xing H 2021 *Phys. Rev. Lett.* **126** 012301
[43] Yun H, Park D, Noh S, Park A, Park W, Cho S, Hong J, Kim Y, Lim S and Lee S H 2023 *Phys. Rev.* C **107** 014906
[44] Cho S *et al* (EXHIC) 2017 *Prog. Part. Nucl. Phys.* **95** 279
[45] Martinez Torres A, Khemchandani K P, Navarra F S, Nielsen M and Abreu L M 2014 *Phys. Rev.* D **90** 114023
[46] Abreu L M, Khemchandani K, Torres A M, Navarra F and Nielsen M 2016 *Phys. Lett.* B **761** 303
[47] Abreu L M, Khemchandani K P, Martínez Torres A, Navarra F S and Nielsen M 2018 *Phys. Rev.* C **97** 044902
[48] Abreu L M, Navarra F S and Nielsen M 2020 *Phys. Rev.* C **101** 014906
[49] Abreu L M 2021 *Phys. Rev.* D **103** 036013
[50] Le Roux C, Navarra F S and Abreu L M 2021 *Phys. Lett.* B **817** 136284
[51] Abreu L M 2022 *PoS XVHadronPhysics* **408** 012

[52] Abreu L M, Navarra F S, Nielsen M and Vieira H 2022 *Eur. Phys. J.* C **82** 296
[53] Abreu L M, Vieira H P L and Navarra F S 2022 *Phys. Rev.* D **105** 116029
[54] Abreu L M, Navarra F S, Nielsen M and Vieira H P L 2023 *Phys. Rev.* D **107** 114013
[55] Britto A L M, Abreu L M and Navarra F S 2023 *Phys. Rev.* D **108** 096028
Abreu L M, Britto A L M, Navarra F S and Vieira H P L 2024 *Phys. Rev.* D **109** 014041
[56] Abreu L M, Navarra F S and Vieira H P L 2024 *Physical Review D* **110** 014011
[57] Cho S and Lee S H 2013 *Phys. Rev.* C **88** 054901
[58] Chen L W, Ko C M, Liu W and Nielsen M 2007 *Phys. Rev.* C **76** 014906
[59] Bracco M, Chiapparini M, Navarra F and Nielsen M 2012 *Prog. Part. Nucl. Phys.* **67** 1019
[60] Oh Y, Song T and Lee S H 2001 *Phys. Rev.* **63** 034901
[61] Carvalho F, Duraes F, Navarra F and Nielsen M 2005 *Phys. Rev.* C **72** 024902
[62] Gamermann D *et al* 2010 *Phys. Rev.* D **81** 014029
[63] Navarra F S, Nielsen M, Marques de Carvalho R S and Krein G 2002 *Phys. Lett.* B **529** 87
Duraes F O, Lee S H, Navarra F S and Nielsen M 2003 *Phys. Lett.* B **564** 97
Abreu L M, Cavalcanti E and Malbouisson A 2018 *Nucl. Phys.* A **978** 107
[64] Cho S and Lee S H 2018 *Phys. Rev.* C **97** 034908
[65] Chen L W, Greco V, Ko C M, Lee S H and Liu W 2004 *Phys. Lett.* B **601** 34
[66] Chen L W, Ko C M, Liu W and Nielsen M 2007 *Phys. Rev.* C **76** 014906
[67] Bjorken J D 1983 *Phys. Rev.* D **27** 140
[68] Ghosh P, Nayak J K, Singh S K and Agarwalla S K 2020 *Phys. Rev.* D **101** 094004
[69] Singh S K, Ghosh P and Nayak J K 2021 *Phys. Rev.* D **104** 034027
[70] Niemi H, Eskola K J, Paatelainen R and Tuominen K 2016 *Phys. Rev.* C **93** 014912
[71] Abreu L M, Navarra F S and Vieira H P L 2022 *Phys. Rev.* D **106** 074028